Redox Biology 24 (2019) 101189

Contents lists available at ScienceDirect

Redox Biology

journal homepage: www.elsevier.com/locate/redox

Dual blockage of STAT3 and ERK1/2 eliminates radioresistant GBM cells

Bowen Xie[a,b,c], Lu Zhang[a,b,c], Wenfeng Hu[a,b], Ming Fan[c], Nian Jiang[c], Yumei Duan[d], Di Jing[c], Wenwu Xiao[e,f], Ruben C. Fragoso[c,f], Kit S. Lam[e,f], Lun-Quan Sun[a,b,**], Jian Jian Li[c,f,*]

[a] Center for Molecular Medicine, Xiangya Hospital, Central South University, Changsha, China
[b] Key Laboratory of Molecular Radiation Oncology Hunan Province, Changsha, China
[c] Department of Radiation Oncology, University of California Davis School of Medicine, Sacramento, CA, 95817, USA
[d] Department of Pathology, Xiangya Hospital, Central South University, Changsha, China
[e] Department of Biochemistry and Molecular Medicine, University of California Davis School of Medicine, Sacramento, CA, USA
[f] NCI-Designated Comprehensive Cancer Center, University of California Davis School of Medicine, Sacramento, CA, USA

ARTICLE INFO

Keywords:
GBM
Radiotherapy
Radioresistance
STAT3
ERK1/2
Tumor regrowth

ABSTRACT

Radiotherapy (RT) is the major modality for control of glioblastoma multiforme (GBM), the most aggressive brain tumor in adults with poor prognosis and low patient survival rate. To improve the RT efficacy on GBM, the mechanism causing tumor adaptive radioresistance which leads to the failure of tumor control and lethal progression needs to be further elucidated. Here, we conducted a comparative analysis of RT-treated recurrent tumors versus primary counterparts in GBM patients, RT-treated orthotopic GBM tumors xenografts versus untreated tumors and radioresistant GBM cells versus wild type cells. The results reveal that activation of STAT3, a well-defined redox-sensitive transcriptional factor, is causally linked with GBM adaptive radioresistance. Database analysis also agrees with the worse prognosis in GBM patients due to the STAT3 expression-associated low RT responsiveness. However, although the radioresistant GBM cells can be resensitized by inhibition of STAT3, a fraction of radioresistant cells can still survive the RT combined with STAT3 inhibition or CRISPR/Cas9-mediated STAT3 knockout. A complementally enhanced activation of ERK1/2 by STAT3 inhibition is identified responsible for the survival of the remaining resistant tumor cells. Dual inhibition of ERK1/2 and STAT3 remarkably eliminates resistant GBM cells and inhibits tumor regrowth. These findings demonstrate a previously unknown feature ofSTAT3-mediated ERK1/2 regulation and an effective combination of two targets in resensitizing GBM to RT.

1. Introduction

GBM remains as a critical clinical issue with the worst prognosis and unacceptable low survival rate after diagnosis [1,2]. RT is one of the major post-surgical modalities for the local control of GBM; however, the efficacy of RT is limited by the tumor adaptive radioresistance. Radioresistant cells in solid tumors including GBM are enriched with cancer stem cells (CSCs) and linked with cancer adaptive resistance [3,4]. CD133, a marker for brain tumor stem cells [5,6], is enhanced in radiation treated GBM [7], and $CD133^+$ GBM cells isolated from human specimens are more efficient in repairing DNA damage than that in $CD133^-$ cells [8]. However, to significantly improve the efficacy of RT in GBM treatment, the molecular insights causing the resistance phenotype of GBM cells are to be elucidated.

STAT3 is a well-defined redox-sensitive oncogenic transcription factor [9–11] and plays a key role in the maintenance of the stemness of $CD133^+$ tumor cells including GBM cells [12,13]. Abundant expression and persistent activation of STAT3 are identified in cancer cells conferring tumor resistance and aggressive progression [14–18]. Anti-tumor treatment-induced STAT3 activation has also been observed in a variety of tumor cells. Therapeutic approaches targeting HER2 [19], EGFR [20,21], MEK-ERK [22], ALK and MET [20] are found to induce

Abbreviations: GBM, glioblastoma multiforme; STAT3, signal transducer and activator of transcription 3; ERK1/2, extracellular signal-regulated kinase 1 and 2; RT, radiotherapy; CSC, cancer stem cell; mTOR, mechanistic target of rapamycin kinase; AKT, AKT Serine/Threonine Kinase 1; CBP, CREB binding protein; RSK-1, ribosomal protein S6 kinase A1; c-fos, FBJ murine osteosarcoma viral oncogene homolog; c-Myc, v-Myc avian myelocytomatosis viral oncogene homolog; Ets-1, v-Ets avian erythroblastosis virus E26 oncogene homolog 1; GSK 3β, glycogen synthase kinase 3 beta; OS, overall survival; RFS, relapse-free survival; WT, wild type; CHX, cycloheximide

* Corresponding author. Department of Radiation Oncology, University of California Davis School of Medicine, Sacramento, USA.
** Corresponding author. Center for Molecular Medicine, Xiangya Hospital, Central South University, Changsha, China.
E-mail addresses: lunquansun@csu.edu.cn (L.-Q. Sun), jijli@ucdavis.edu (J.J. Li).

https://doi.org/10.1016/j.redox.2019.101189
Received 18 February 2019; Received in revised form 17 March 2019; Accepted 1 April 2019
Available online 09 April 2019

STAT3 activation causing tumor adaptive resistance. In addition, radiation promotes STAT3 activation and nuclear translocation to enhance GBM malignancy [23]. Considering the important roles in maintaining the stemness and enhancing radioresistance of tumor cells [24], STAT3 is a promising target with increasing specific inhibitors being invented and entered in clinical trials for treatment of diverse human cancers, including being developed to enhance temozolomide-mediated radiosensitization [25]. However, the specific efficacy of targeting STAT3 in the treatment of radioresistant GBM rumors remains unclear.

ERK1/2 is another fundamental pro-surviving factor in mammalian cells. Increasing evidence suggests that ERK1/2-dependent RAF/MEK/ERK1/2 pathway is essential in promoting tumor progression and mediating resistance to anti-tumor therapies by various mechanisms [26]. Recently, RAF inhibition-mediated ERK activation similar to therapies-induced STAT3 feedback loop activation is linked with tumor growth [27]. It has been reported that ERK1/2 enhances STAT3 Serine727 phosphorylation whereas dephosphorylates STAT3 at Tyrosine 705 [28]. In addition to Serine727, ERK1/2 phosphorylates STAT3 on other two serine residues involving in the reduction of tyrosine705 phosphorylation and DNA binding activity [29]. As such, although ERK1/2 signaling pathway has been extensively studied, it remains unclear whether pSTAT3 (Y705) affects ERK1/2 activation in tumor cells, especially in radioresistant GBM cells.

Here we reveal that activation of STAT3 is predominantly enhanced in CD133-enriched radioresistant GBM cells and recurrent tumors. However, surprisingly, although blocking of STAT3 increases the sensitivity of resistant GBM cells to radiation, STAT3 inhibition-mediated ERK1/2 activation promotes cell survival and repopulation under radiation treatment. A synergetic administration of ERK1/2 inhibitors can effectively eliminate resistant GBM cells and suppress GBM tumor regrowth post RT. As such, we demonstrate that a combinational inhibition of STAT3 and ERK1/2 may be a novel and efficient strategy for GBM radiotherapy.

2. Materials and methods

2.1. Cell lines and culture conditions

Human GBM U251 and U87 cells, breast cancer MCF7 and MDA-MB-231 cells were purchased from ATCC. U251 cells were maintained in MEM medium (CORNING Cellgro, Catalog # 10-010-CV) containing 10% FBS (CORNING, Catalog # 35-010-CV), 0.1 mM NEAA (CORNING Cellgro, Catalog # 25-025-CI), 1 mM sodium pyruvate (CORNING Cellgro, Catalog # 25-000-CI) and 10 mM Hepes (VWR, Catalog # 97064-360); U87, MCF7 and MDA-MB-231 cells were maintained in DMEM medium (CORNING Cellgro, Catalog # 10-013-CV) with 10% FBS. Human astrocytes HA1800 were maintained in DMEM supplemented with 10% FBS. Radioresistant clones of U251 or U87 cells were derived from the corresponding wild-type cells after a chronically irradiation (2 Gy per workday for 20 days) and cells from U251/C7 were verified with radioresistance and used as radioresistant cells in the subsequent experiments, medium formula for maintaining radioresistant cells was the same as the parental cells. Radioresistant H157R and H358R cells were kindly gifted from Xingming Deng (Winship Cancer Institute of Emory University) [30] and were maintained in RPMI-1640 medium (Hyclone) with 10% FBS.

2.2. Antibodies and reagents

Antibodies used in this study wereCD133 (IHC: BOSTER, PA2049; WB, Miltenyi Biotec, 130-092-395), pSTAT3 (Y705) (IHC, IF, IP and WB: Cell Signaling Technology, 9145), STAT3 (WB: Cell Signaling Technology, 4904), pERK1/2 (IHC, IF and WB: Cell Signaling Technology, 4370), CBP (WB: Santa Cruz Biotechnology, sc-369), RSK-1 (WB: Santa Cruz Biotechnology, sc-231), c-Myc (WB: Cell Signaling Technology, 9402s), c-fos (WB: Santa Cruz Biotechnology, sc-253), Ets-1 (WB: Santa Cruz Biotechnology, sc-111), *p*-GSK 3β (Ser9) (WB: Cell Signaling Technology, 5558), GSK 3β (WB: Cell Signaling Technology, 9315s), ERK1/2 (IP and WB: Cell Signaling Technology, 4695), phospho-mTOR (Ser2448) (WB: Cell Signaling Technology, 2971), mTOR (WB: Cell Signaling Technology, 2983), phospho-AKT (Ser473) (WB: Cell Signaling Technology, 9271), AKT (WB: Cell Signaling Technology, 9272), α-tubulin (Sigma-Aldrich, T6074), rabbit IgG (IP: Santa Cruz Biotechnology, sc-2027), anti-rabbit IgG (WB: Cell Signaling Technology, 7074s) anti-mouse IgG (WB: Cell Signaling Technology, 7076s).

Selective pSTAT3 (Y705) inhibitors Cryptotanshinone (Catalog #S2285), S3I-201 (Catalog #S1155), Stattic (Catalog #S7024), WP1066 (Catalog #S2796), STAT1 activation inhibitor Fludarabine (Catalog #S1491), MEK1/2 inhibitors U0126 (Catalog #S1102) and Selumetinib (AZD6244, Catalog #S1008) were purchased from Selleckchem. Anexin IV (Catalog # ANNEXINV01-3) was bought from CaltagLaboratories, propidium iodide (PI, Catalog #L7010) was bought from Invitrogen. Cycloheximide (CHX, Catalog #C7698) and dimethyl sulfoxide (DMSO, Catalog #D2650) were bought from Sigma-Aldrich. DAPI Fluoromount-G (Catalog # 0100-20) was bought from SouthernBiotech.

2.3. Immunoprecipitation and immunoblotting analyses

Proteins extracted with a modified buffer from cells were followed by immunoprecipitation and immunoblotting detection with corresponding antibodies, as previously described [31]. Three independent experiments were done in triplicate.

2.4. Luciferase reporter gene assay

Transcriptional activation of STAT3 in GBM cells was measured as previously described except for slight modifications that no cytokine treatment was applied in this study [32]. Three independent experiments were performed in triplicate.

2.5. Immunohistochemical analysis

Mouse tumor tissues were fixed and prepared for immunohistochemistry (IHC) or haematoxylin and eosin (HE) staining. For IHC analysis, the specimens were stained with antibodies against CD133, pY705-STAT3, pERK1/2 or cleaved-caspase 3. For HE analysis, the specimens were stained with Mayer's haematoxylin and subsequently with eosin (Biogenex Laboratories).

The tissue sections from paraffin-embedded 34 paired human GBM specimens were stained with an antibody against CD133 or pY705-STAT3. 3–5 sections of each sample and 5–6 high-power fields (HPF) of each section were used for analysis and quantification. The tissue sections were quantitatively scored according to the staining intensity (0, negative; 1, slight yellow; 2, brown; 3, dark brown) and percentage of positive stained cells (0, ≤10%; 1, 10%–25%; 2, 25%–50%; 3, 50%–75%; 4, ≥75%) with a scoring scale ranging from 0 to 12, protein expression in tumor tissues was graded as negative (0); low/weak (1–4); moderate (5–8); high/strong (9–12), respectively. Scores of recurrent samples were compared with the corresponding primary counterparts from the same patients, of which 27 out of 34 patients received post-surgical RT. The use of human brain tumor specimens and database was approved by Human Ethic Committee of Xiangya Hospital of Central South University. In determining the effects of treatments on the indicated proteins in xenografts, alterations of the percentage of positive cells in mice tumor tissues before or after treatments were employed instead of H-score. Similarly, 3 sections of each tumor and 5–6 HPF of each section were used to count the percentage of protein-expressing cells (no staining, negative; slight yellow, brown or dark brown, positive).

2.6. CRISPR/Cas9-based STAT3 knockout

The sgRNAs were designed following the instruction published by Dr. Zhang Lab's CRISPR design software (http://crispr.mit.edu) and the established protocol that has been described in previous publication [33]. Six oligos were designed corresponding to the human sgRNAs were synthesized and cloned into lentiCRISPR v2 vectors from the Addgene plasmid repository (plasmid#52961) following the Zhang Lab GeCKO pooled library amplification protocol. To minimize the possibility of nonspecific targeting, three sgRNAoligos of each targeting gene were synthesized and tested. The sgRNA with the best knockout efficiency determined by western blotting was chosen for the subsequent experiments. The sgRNA sequences are as follows:

LentiCrispr V2/hSTAT3gRNA #1 (032) F: CACCGATCGGCCGGTG CTGTACAAT

LentiCrispr V2/hSTAT3gRNA #1 (032) R: AAACATTGTACAGCAC CGGCCGATC

LentiCrispr V2/hSTAT3gRNA #2 (033) F: CACCGACGCCGGTCTT GATGACGAG

LentiCrispr V2/hSTAT3gRNA #2 (033) R: AAACCTCGTCATCAAG ACCGGCGTC

LentiCrispr V2/hSTAT3gRNA #3 (034) F: CACCGGTGATACACCTC GGTCTCAA

LentiCrispr V2/hSTAT3gRNA #3 (034) R: AAACTTGAGACCGAGG TGTATCACC

The lentiviral particles were generated using 293T cells following the protocol from Addgene. For gene editing, U251/C7 cells were trypsinized into single cell suspension and were plated 1.25×10^5 cells/0.5 ml per well in 12-well plates. 1 ml of virus-containing supernatant with 10 ng polybrene (Sigma-Aldrich, Catalog #H9268-10G) was added to the cells 12 h after incubation. Then, 0.5 ml additional regular medium containing 10% heat-inactive FBS was added 6 h after incubation and cultured for overnight. The infection medium was replaced with 2 ml fresh medium with 10% FBS and cultured for 72 h. Cells were passaged to 60 mm dishes and selected by culturing in 0.3 μg/ml puromycin for 1 week and the knockout of targeted gene was verified by immunoblotting.

2.7. Establish cell lines expressing wild-type or mutant STAT3

The expression plasmids, Wild-type STAT3, mutant STAT3 (Y705F), and control vectors were kindly provided by T Hirano [34]. 5×10^5 U251/clone7 cells in 6-well plate were transfected with 1 ml wild-type STAT3 or STAT3 (Y705F) virus medium containing 80 μg/ml polybrene, similarly as previously described [34]. After 6 h, 0.5 ml fresh complete medium was added to cells followed by further 10 h incubation, then replace with fresh medium. 1 μg/ml puromycin was added to cells in 24 h for 1 week to select out resistant cells. The expression of wild-type STAT3 and mutant STAT3 Y705F in cells were determined by immunoblotting.

2.8. Tumor sphere formation assay

Cells were sieved with 40 μm cell strainers (Fisher) and single-cell suspensions were seeded into low-attachment 60 mm Petri dishes at a density of 500 cells/ml. Cells were grown in serum-free MEM medium, supplemented with B27 (Life Technology), 20 ng/ml EGF (Biovision), 20 ng/ml basic-FGF, and 4 μg/ml heparin (VWR). Cells were cultured for 5 days and tumor spheres were counted, sphere size were measured and calculated under light microscopy and collected for further experiments. Three independent experiments were done in triplicate.

2.9. Apoptosis analyses

For Sub-2N analysis, 2×10^5-trypsinized cells were collected and washed with PBS twice. Add 100 μl incubation buffer (1× PBS containing 0.5% BSA) to resuspend pellets. Then cells were stained with 5 μl propidium iodide by 10 min incubation at room temperature (keep in dark) and 100 μl incubation buffer was added to cells before cell death was analyzed using a variation of a conventional FACS method (Millipore, Temecula, CA, USA) to detect sub-2N DNA content which represents cells undergoing apoptosis [35,36]. For Annexin-V/PI staining, U251/C7 cells were incubated with DMSO, cryptotanshinone, selumetinib, U0126, cryptotanshinone plus selumetinib or cryptotanshinone plus U0126 for 4 h, followed with 5 Gy radiation exposure and kept in incubator for additional 48 h. Cells in supernatant and in adherent growth were collected and washed with PBS twice, then stained with Annexin-V/PI. Cell death was determined by FCA and analyzed with FlowJo.

2.10. Kaplan-Meier survival analyses

TCGA RNA-seq data for GBM, gliomas and breast cancer samples were obtained from UCSC Xena browser (http://xena.ucsc.edu/). The overall survival and relapse-free survival were evaluated using the Kaplan–Meier method, and statistical differences in survival times were determined using the log-rank test as described elsewhere. The cohort include 720 lung adenocarcinoma samples obtained from Kaplan-Meier Plotter (http://kmplot.com/analysis/index.php?p=service&cancer=lung) were used to generate the overall survival analyses of lung adenocarcinoma based on STAT3 (Affy ID, 208992_s_at) status. A log rank test was used to test for differences of more than one survival curve.

2.11. In vivo experiments

2.11.1. Orthotopic model

NSG mice aged 6 weeks were obtained from The Jackson Laboratory (Stock No: 005557). The animal use and care protocol of in vivo RT was approved by the Institutional Animal Use and Care Committee of the University of California Davis (IACUC 15315). For orthotopic xenografts, wild-type U251 cells were trypsined, washed twice with PBS and resuspended in PBS (5×10^6 cells/50 μl) for the following use. NSG mice (n = 3 per group) were anesthetized with ketamine and xylazine. 5 μl of 5×10^5 U251 cells were stereotactically and intracranially injected through an entry site located 1.5 mm posterior to the bregma and 1.5 mm to the right of the sagittal suture to a depth of 2.5 mm below the surface of the skull using a 10-μL Hamilton syringe. Tumors developed 8 days after cell injection, and mice were received 2 Gy/day local RT for 5 days (day 8, day 9, day 10, day 11 and day 12). Magnetic Resonance Imaging (MRI) examinations of mice brain were performed at day 8, day 20 and day 58 after cell injection.

2.11.2. Subcutaneous model

For the subcutaneous tumor inoculation, 5×10^6 wild-type U251 cells in 200 μl PBS were injected into 6 weeks old female nude mice (The Jackson Laboratory, Stock No: 002019) in the right flanks (n = 7 per group). Tumor volumes were estimated and calculated using the formula for a spheroid: V = Length x width^2/2. Tumors were protruded for fractionated irradiation (2 Gy/day) when tumor volumes reached approximately 200 mm^3 (tumors received radiation at day 16, day 17, day 18, day 19 and day 20, respectively). Tumor volumes shrank but re-reached approximately 200 mm^3 8 days after RT, and the regrowing tumors were used as radioresistant tumors. Cryptotanshinone (25 mg/kg, 20 mg/ml in 25 μl DMSO), selumetinib (25 mg/kg, 20 mg/ml in 25 μl DMSO) or cryptotanshinone combined with selumetinib was then intratumorally injected 4 h before tumors receiving RT (2 Gy/day for 2 days). The inhibitors were administered every other day till the end of experiment. Tumor volumes were estimated and calculated at the indicated times.

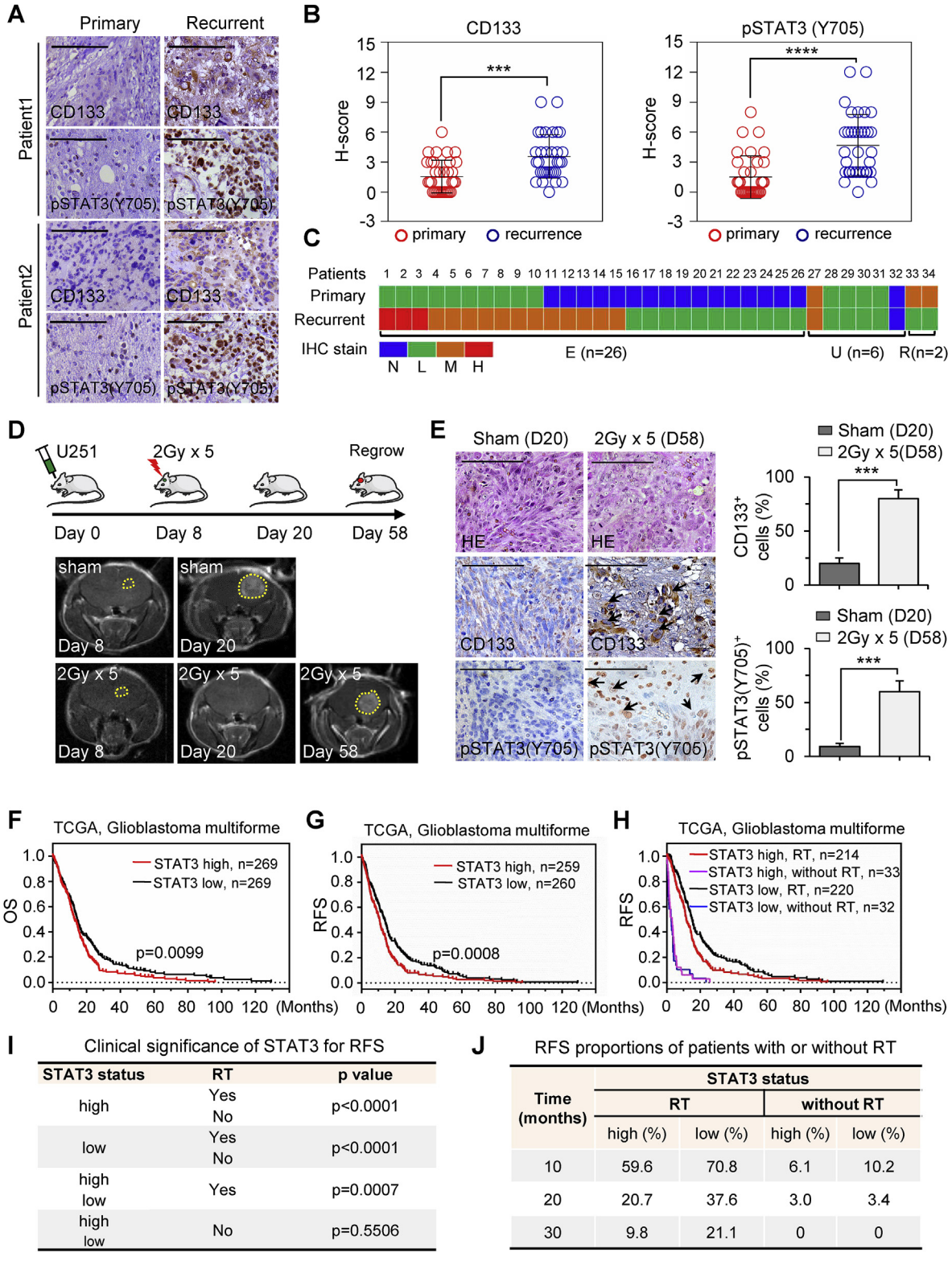

I Clinical significance of STAT3 for RFS

STAT3 status	RT	p value
high	Yes No	p<0.0001
low	Yes No	p<0.0001
high low	Yes	p=0.0007
high low	No	p=0.5506

J RFS proportions of patients with or without RT

Time (months)	STAT3 status			
	RT		without RT	
	high (%)	low (%)	high (%)	low (%)
10	59.6	70.8	6.1	10.2
20	20.7	37.6	3.0	3.4
30	9.8	21.1	0	0

Fig. 1. Activation of STAT3 correlates with GBM radioresistance. (**A**) Representative IHC staining of pSTAT3 (Y705) and CD133 in paired primary and recurrent tumors. Scale bar, 100 μm. (**B**) IHC scores distribution of pSTAT3 (Y705) (right) and CD133 (left) in 34 paired (primary and recurrent tissues from the same patient) tumors. Mean ± SD, ***$P < 0.001$, ****$P < 0.0001$. (**C**) Related pSTAT3 (Y705) expression levels evaluated by N-H scales (N, negative; L, low; M, moderate; H, high). E, enhanced; U, unchanged; R, reduced. (**D**) Above, orthotopic U251 xenograft tumors treated by local radiation with 2 Gy daily for 5 days, sham radiation was used as control. Bottom, MRI imaging of mice brain at day 8, day 20 or day 58. (**E**) Left, representative HE and IHC of CD133 and pSTAT3 (Y705) in sham or regrown orthotopic GBM tumors. Right, quantification of CD133 and pSTAT3 (Y705) in sham and regrown tumors. Mean ± SD, ***$P < 0.001$. (**F**) Kaplan-Meier estimates of the overall survival (OS) of GBM patients from TCGA related to STAT3 transcript levels. (**G**) Kaplan-Meier analysis of the relapse-free survival (RFS) of TCGA patients based on transcriptional STAT3expression status (high expression, red line, n = 259; low expression, black line, n = 260). $P = 0.0008$. (**H**) Kaplan-Meier analysis of GBM patients with or without RT whose tumor expressed high or low STAT3. (**I**) Statistically significant difference in (**H**). Patients with different STAT3 status treated with or without RT were analyzed. (**J**) RFS proportions at 10, 20 or 30 month of patients in (H).

2.12. Statistical analysis

Data in this study are presented as mean ± SD, and analyzed using the two-tailed Student *t*-test for two groups or ANOVA for multiple groups. The statistical significance of Kaplan–Meier survival curves was assessed with a Mann-Whitney test. A value of p less than 0.05 was considered as statistically significant. $^{*}P < 0.05$, $^{**}P < 0.01$, $^{***}P < 0.001$.

3. Results

3.1. STAT3 activation is enhanced in recurred GBM tumors and diverse radiation-survived tumor models

To examine whether activation of STAT3 (pSTAT3 Y705) was related to the radioresistance and recurrence of GBM tumors, we firstly analyzed 34 paired clinical GBM samples of both primary and recurrent tumors from the same patients; most of them received RT. pSTAT3 (Y705) was enhanced in recurrent tissues (26 out of 34 patients, 76.5%) compared with their corresponding primary counterparts (Fig. 1A–C and Supplementary Table 1). In addition, more than 90% of recurrent tumors were positive in both CD133 and pSTAT3 (Y705) (Supplementary Table 2). Indicating that pSTAT3 (Y705) is potentially related to GBM radioresistance and recurrence.

Based on this result, to further explore the dynamic features of STAT3 in GBM response to radiation, we employed two approaches. First, NSG mice were intracranially injected with wild-type U251 cells and followed by sham or fractionated local radiation at day 8 post inoculation. The tumors received radiation treatment shrunk at day 20 and regrowth was observed at day 58 (Fig. 1D). In consistence with the increase of CD133 and pSTAT3 (Y705) in recurrent clinical GBM tissues, the regrown GBM xenografts in mouse brains showed enhanced CD133 and pSTAT3 (Y705) staining compared with the parallel tumors received sham RT (Fig. 1E). Second, we established diverse in vitro models to monitor the dynamic alteration of pSTAT3 (Y705) in tumor cells before and after receiving clinically mimic fractionated ionizing radiation (2 Gy per workday for 20 days). The cells from 6 out of 7 survived U251 clones revealed significant enhancement of CD133 and pSTAT3 (Y705) expression compared to the parental cells (Supplementary Figs. 1A and B). Among the CD133-expressing cells, clone7 (U251/C7) showed the highest enrichment of pSTAT3 (Y705) and were more aggressive and radioresistant comparing with the parental counterparts (Supplementary Figs. 1C–E). Similarly, we observed enhancement of STAT3 activation and CD133 expression in U87 clones survived chronic radiation as U251 cells (Supplementary Fig. 1F). Analogously, pSTAT3 (Y705) was induced in breast cancer MCF7 cells, lung cancer H358 and H157 cells after fractionated radiation (Supplementary Fig. 1G). In addition to the changes of molecular characteristics, the survived clones of U251 and U87 exhibited more 'aggressive' morphology, which was completely different from their parental cells, except U251/C1, the only survived clone that shows no increase of STAT3 activation (Supplementary Figs. 1H and I). Recent studies have revealed the relationship between therapeutic resistance and cell morphology alterations [37]. Thus, the morphology plasticity of GBM cells survived radiation may represent a dominant phenotype in adaptation to rewired molecular circuit. Moreover, similar median STAT3 expression was observed in over 30 GBM cell lines including U251 and U87 cells compared with clinical GBM tumors, both of which were much higher than that in normal brain tissues (Supplementary Figs. 2A and B). Thus, together with literatures [38,39], these data strongly suggest that STAT3 correlates with the malignancy and radioresistance of GBM tumors.

3.2. STAT3 is associated with poor prognosis in GBM

Since recurrent clinical GBM tissues and recurred orthotopic GBM tumors demonstrated robust STAT3 activation compared with the corresponding primary counterparts and sham-irradiated tumors, respectively, we next uncovered the relationship between STAT3 expression and GBM prognosis. We performed Kaplan-Meier survival analysis of GBM patients in TCGA based on STAT3 status. Comparing with low STAT3 expression in tumor tissues, high levels of STAT3 were positively associated with poorer overall survival (OS) ($P = 0.0099$) in general (Fig. 1F). Particularly, patients with high STAT3 expression achieved OS by 63.6%, 24.5% and 8.8% at 10, 20 and 30 months, respectively, while the OS of those with low STAT3 expression was correspondingly 67.7%, 36.4% and 19.5% (Supplementary Fig. 2C). Similar significant difference was observed in relapse-free survival (RFS) between patients with high or low expression of STAT3 ($P = 0.0008$) (Fig. 1G and Supplementary Fig. 2D).

To further determine the correlation between STAT3 expression and GBM radioresistance, we analyzed the effect of STAT3 on the radiation response of GBM based on the clinical information from TCGA database. Almost no difference of RFS probability was observed in patients without RT probably due to the short median survival time, while improved RFS was obtained in patients received RT ($P < 0.0001$) (Fig. 1H and I). However, importantly, patients with elevated STAT3 expression had significantly reduced RFS (59.6%, 20.7% and 9.8% at 10 month, 20 month and 30 month, respectively) compared with those expressing low STAT3 (achieved 70.8%, 37.6% and 21.1% of RFS proportions at 10 month, 20 month and 30 month, respectively) ($P = 0.0007$) (Fig. I and J). Similarly, STAT3 status was also linked to prognostic significance for the OS of patients with glioma ($P = 1.84 \times 10^{-13}$), breast cancer ($P = 0.0005$) or lung adenocarcinoma ($P = 4.9 \times 10^{-6}$) (Supplementary Fig. 2E).

3.3. Radioresistant GBM cells survive radiation in the presence of STAT3 inhibition

To further examine the effect of radiation on STAT3 in GBM, we performed a range of tests in several relevant in vitro systems, and found that STAT3 activation was inducible in radioresistant GBM cells by radiation stimulation (Fig. 2A). STAT3 activation could be efficiently inhibited by specific inhibitors including cryptotanshinone (inhibition of phosphorylation of STAT3 tyrosine705; Supplementary Fig. 3A) [40], an inhibitor extracted from Danshen, which has been used as an Asian medicine in cardiovascular disorders [41]. And subsequently radioresistant U251/C7 cells were used to test the blocking efficacy of STAT3 transcriptional activity and radiation sensitization. Cells were incubated with cryptotanshinone, or other STAT3 inhibitors including WP1066 [42,43] (inhibition of JAK2 and STAT3 activation) and S3I-201 [44,45] (inhibition of phosphorylation of STAT3 tyrosine 705 and its DNA-binding activity) in the presence or absence of 5 Gy radiation treatment (Fig. 2B and C). Though blocking STAT3 activation reduced the clonogenicity of U251/C7 cells, we observed that 10%–30% cells could not be eradicated by the combinational treatment with radiation and STAT3 blockade. For further confirmation, we knocked out STAT3 in U251/C7 cells via CRISPR/cas9-mediated gene editing (Fig. 2D) and exposed cells to 5 Gy radiation. Likewise, comparing with STAT3-expressing control cells, the clonogenic survival of STAT3-deficient $CD133^{+}$ cells reduced to 12%～22% which was doggedly preserved for repopulation (Fig. 2E). These reductions could be rescued by reconstitution with wild-type STAT3, but not with re-expressing dominant negative mutant STAT3 (Y705F, tyrosine705 to Phenylalanine 705) (Fig. 2F). In addition, we observed that removal of STAT3 inhibitor roused the well-preserved proliferative capability of cells retarded with STAT3 blockade (Supplementary Fig. 3B). Interestingly, despite of reduced spheres number, U251/C7 cells formed loose spheres with larger size in the presence of STAT3 inhibitor cryptotanshinone (Supplementary Fig. 3C).

We had observed that a small portion of adherent U251/C7 cells detached within 24 h after exposure to STAT3 inhibitors. These

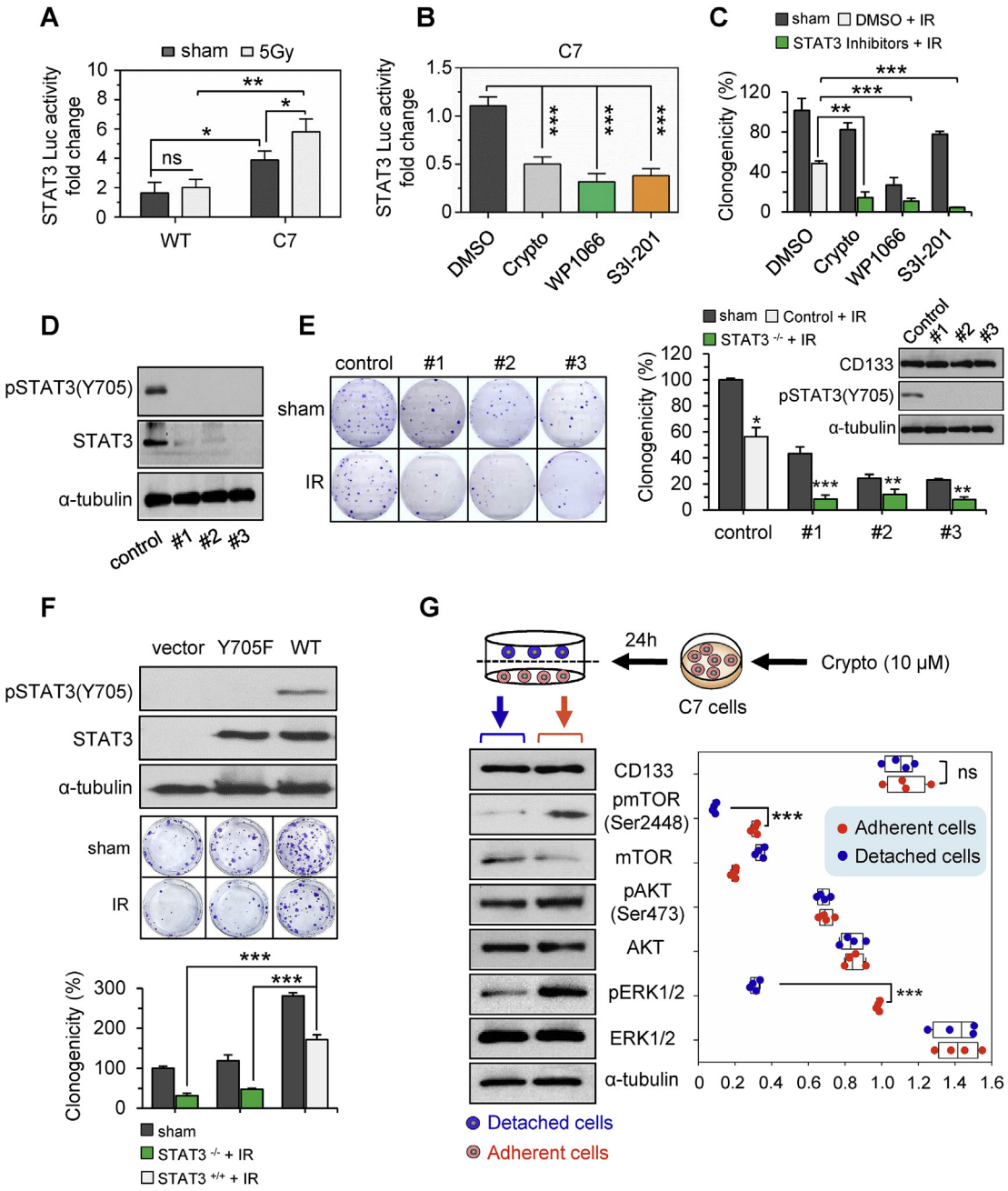

Fig. 2. A fraction of radioresistant GBM cells survives STAT3 inhibition with ERK1/2 activation. (**A**) STAT3 luciferase reporter activity in wild-type and radioresistant U251/C7 cells 24 h after sham or 5 Gy radiation. Mean ± SD, $*P < 0.05$, $**P < 0.01$; ns, no significance. (**B**) STAT3 reporter activity in U251/C7 cells 24 h after incubation with DMSO, Cryptotanshinone (Crypto, 10 μM; STAT3 inhibition), WP1066 (5 μM; STAT3 inhibition) or S3I-201 (50 μM; STAT3 inhibition). Mean ± SD, $***P < 0.001$. (**C**) Clonogenic survival of U251/C7 cells treated with sham or 5 Gy IR and cryptotanshinone (10 μM), WP1066 (5 μM) or S3I-201 (50 μM). Mean ± SD, $**P < 0.05$, $***P < 0.001$. (**D**) Confirmation of STAT3-deficient cell lines (#1, #2 and #3) generated by CRISPR/cas9-mediated knockout in U251/C7 cells. (**E**) Left, representative image of surviving clones of STAT3-knockoutcells (#1, #2 and #3) with or without IR (5 Gy). Right, quantification of the surviving clones (Insert, immunoblotting of CD133 and pSTAT3 (Y705) in indicated surviving clones). Mean ± SD, $*P < 0.05$, $**P < 0.01$, $***P < 0.001$. (**F**) Clonogenic survival of STAT3-knockout #3 cells rescued with vector, mutant STAT3 (Y705F, tyrosine to Phenylalanine) or wild-type STAT3 and treated with sham and 5 Gy IR. Mean ± SD, $***P < 0.001$). (**G**) U251/C7 cells were exposed to cryptotanshinone (10 μM) for 24 h, the detached cells and adherent cells were then collected for protein extraction, separately (above schematic). CD133, phosphorylated mTOR (Ser2448), AKT (Ser473) and ERK1/2 were detected by western blot (bottom left) and quantified by ImageJ for 4 times (bottom right) and normalized to α-tubulin. Data are representative of three independent experiments. Mean ± SD, $***P < 0.001$; ns, no significance.

detached cells could not re-adhere by refreshing with complete medium. It seemed reasonable to propose that the detached cells were more sensitive to STAT3 inhibition than those of adherent cells. To understand the underlying mechanisms, we incubated U251/C7 cells with cryptotanshinone for 24 h, the detached and adherent cells were then collected respectively and extracted for proteins immediately. Interestingly, the phosphorylated mTOR (Serine2448) and ERK1/2 (Threonine 202/tyrosine 204), two of the well-studied essential factors persistently activated in multiple tumors and interplayed with STAT3 for tumor survival, were both increased by more than 3 folds in adherent cells compared to detached cells while CD133 and phosphorylated AKT (Ser473) almost remain the same levels (Fig. 2G).

Hyperresponsive ERK1/2 signaling was reported to phosphorylate mTOR at serine2448 via S6K1 to regulate cell growth and survival [46]. Our data suggest that, despite STAT3 inhibition increases the sensitivity of partial resistant cells to radiation treatment, a proportion of cells can endure combinational treatment of radiation and STAT3 inhibition potentially due to the activation of other molecular pathways, at least ERK1/2 signaling.

3.4. ERK1/2 activation mediates resistance to STAT3 inhibition in radioresistant GBM cells

To investigate whether inhibition of STAT3 leads to activation of ERK1/2 pathway, we first tested the basal phosphorylated ERK1/2 (pERK1/2) in orthotopic xenografts. IHC staining shows that pERK1/2 was higher in wild-type tumors [pSTAT3 (Y705) low] than that in tumors regrown from fractionated RT [pSTAT3 (Y705) high)] (Supplementary Fig. 4A). Also, comparing with normal brain tissues, GBM tumors exhibited reduced expression of ERK1/2 and upstream kinases, increased STAT3 and STAT3 downstream genes expression (Supplementary Fig. 4B). To further determine whether STAT3 inhibition affected ERK1/2 activity, U251/C7 cells were challenged with cryptotanshinone. Comparing with DMSO incubation, exposure to cryptotanshinone immediately and significantly enhanced ERK1/2 phosphorylation, which was observed at 0.5 h post treatment and sustained to 24 h (Fig. 3A and Supplementary Fig. 5A). Implying that pSTAT3 (Y705) inhibition-mediated enhancement of ERK1/2 phosphorylation may not depend on the transcriptional activity of pSTAT3 (Y705). Once pSTAT3 (Y705) was blocked, the nuclear translocation of active ERK1/2 was increased (Fig. 3B). Similar increase of ERK1/2 phosphorylation was ascertained in U251/C7 cells treated with other STAT3 inhibitors, such as SH5-07, S3I-201, stattic and WP1066, whereas no alterations of ERK1/2 phosphorylation were observed in those treated with DMSO or STAT1 inhibitor fludarabine (Fig. 3C). In addition to U251/C7 cells, the ERK1/2 phosphorylation in other radioresistant GBM cells such as U87/S8, and radioresistant breast cancer MCF7-R cells as well as lung cancer H358-R and H157-R cells could also be enhanced by STAT3 inhibition (Supplementary Fig. 5B). However, the activation of ERK1/2 cannot be induced by STAT3 inhibition in wild-type U251 and U87 cells, as well as wild-type U251 tumors in which the basal pSTAT3 (Y705) stayed at low levels (Supplementary Figs. 5C–E).

To exclude possible off-target effects of the inhibitors, we transfected U251/C7 cells with vector, STAT3 (Y705F) mutant or STAT3 WT (Supplementary Fig. 5F), followed by 5 Gy radiation treatment. No difference of the basal ERK1/2 activation was observed in the three different cell lines. However, pERK1/2 was significantly increased in cells expressing STAT3 (Y705F) by radiation stimulation, while no alteration was found in those expressing endogenous STAT3 or transfected with wild-type STAT3 (Fig. 3D), suggesting that the mutant STAT3 (Y705F) competitively blocked the endogenous pSTAT3 (Y705)-mediated inhibition of ERK1/2 activation. However, cells overexpressing wild-type STAT3 were reversely increased with pERK1/2 by inhibition of pSTAT3 (Y705), and the enhancement of pERK1/2 was even higher than that in control cells in a time-dependent manner as observed in H358-R and H157-R cells (Fig. 3E and Supplementary Fig. 5G).

To determine how the increased pERK1/2 is generated, we employed Cycloheximide(CHX) to block protein synthesis in the presence or absence of STAT3 inhibition. CHX alone reduced pSTAT3 (Y705) and increased pERK1/2. Interestingly, pERK1/2 was further enhanced in cells with an additional CHX administration whereby protein synthesis inhibition combined with STAT3 inhibition completely depleted pSTAT3 (Y705), indicating that the increased pERK1/2 with STAT3 blockade was originally modified from existing ERK1/2, not from newly expressed proteins. In addition, ERK1/2 was further activated by enhancing pSTAT3 (Y705) inhibition (Fig. 3F). Since ERK1/2 signaling plays a critical mechanism for cell survival, we next blocked pSTAT3 (Y705) in U251/C7 cells and tested downstream proteins of ERK1/2 signaling including CBP, RSK-1, c-fos, c-Myc, Ets-1 and pGSK 3β (Ser9) indicating that c-fos and c-Myc were significantly upregulated. Consistently, phosphorylated GSK 3β (Ser9), the inactive form of GSK 3β known to upregulate β-catenin to promote tumor progression, was also increased after STAT3 depletion, whereas these upregulations can be reversely blocked by an additional ERK1/2 inhibition (Fig. 3G).

Considering ERK1/2 phosphorylation enhancement occurred no longer than 0.5 h after cells incubated with STAT3 inhibitors, mutant STAT3 (Y705) competitively impede wild-type STAT3-mediated ERK1/2 phosphorylation inhibition, and ERK1/2 activation increased by enhancing the depletion of pSTAT3 (Y705), this information strongly suggest that a complex consists of components containing at least pSTAT3 (Y705) and ERK1/2 may exist in radioresistant cells. Although STAT3 was previously reported to physically associate with ERK1/2 [29,47], it is not clear if pSTAT3 (Y705) can form complex with ERK1/2 in radioresistant GBM cells. Coimmunoprecipitation assay showed that inhibition of pSTAT3 (Y705) markedly reduced its binding to ERK1/2 following with rapid increase of ERK1/2 phosphorylation (Supplementary Figs. 6A and B). Collectively, these results suggest that STAT3 inhibition releases ERK1/2 from the complex for phosphorylation to induce downstream oncogenic signaling as a potential compensation bypass for tumor cell survival.

3.5. Dual blockade of STAT3 and ERK1/2 sensitizes GBM cells to radiation in vitro and in vivo

To evaluate whether inhibition of both STAT3 and ERK1/2 could achieve a more efficient anti-radioresistant effect in GBM, we seeded U251/C7 cells for 24 h, and supplemented with medium containing STAT3 inhibitors cryptotanshinone, WP1066 or S3I-201 combined with or without MEK1/2 inhibitor U0126. Compared with cells administered with STAT3 inhibitors alone, cells challenged with a combination treatment of STAT3 and ERK1/2 inhibition were almost completely eliminated by radiation, in which both of pSTAT3 (Y705) and pERK1/2 were almost depleted (Fig. 4A and B and Supplementary Fig. 7A). Since STAT3 inhibitors may have off-target effects, we employed STAT3-knockout #2 and #3 cells derived from U251/C7 to verify the effect. #3 cells were rescued with vector, mutant STAT3 (Y705F) or wild-type STAT3, respectively. And #2 cells were rescued with STAT3 (Y705F) or wild-type STAT3. Each of them was exposed to DMSO, MEK1/2 inhibitors U0126 or selumetinib followed by sham or 5 Gy radiation treatment. Consistently, in the presence of inhibitors of ERK1/2 signaling, radiation completely eradicated the STAT3 knockout cells reconstituted with vector or STAT3 (Y705F). In the absence of ERK1/2 inhibition, radiation could not efficiently eliminated cells, especially those expressing wild-type STAT3 (Fig. 4C).

We next examined the effect of STAT3 and ERK1/2 inhibition on apoptosis induced by radiation. Cells were exposed to 5 Gy radiation plus cryptotanshinone to inhibit STAT3 activation for 48 h. Agreeing with the cell morphology alteration shown in Supplementary Fig. 7B, cell death was increased by radiation from 6.14% (sham) to 11.56% (5 Gy) in the absence of cryptotanshinone, while increased from 14.31% (sham) to 19.13% (5 Gy) in the presence of STAT3 inhibition, suggesting that STAT3 inhibition synergized with radiation to slightly increase cell death. Importantly, cell death could be significantly enhanced from 35.45% (sham) to 43.78% (5 Gy), or 24.97% (sham) to 29.53% (5 Gy) via an additional ERK1/2 inhibition. No significant difference was observed in cell death between DMSO incubated cells and those applied selumetinib (from 7.63% to 14.98%) or U0126 (from 7.5% to 15.58%) alone (Fig. 4D and E and Supplementary Fig. 7C). These observations were further confirmed by measuring the level of cleaved-caspase3 (Fig. 4F). Taken together, our results indicate that blocking STAT3 inhibition-induced ERK1/2 activation could achieve a more efficient eradication of radioresistant GBM cells.

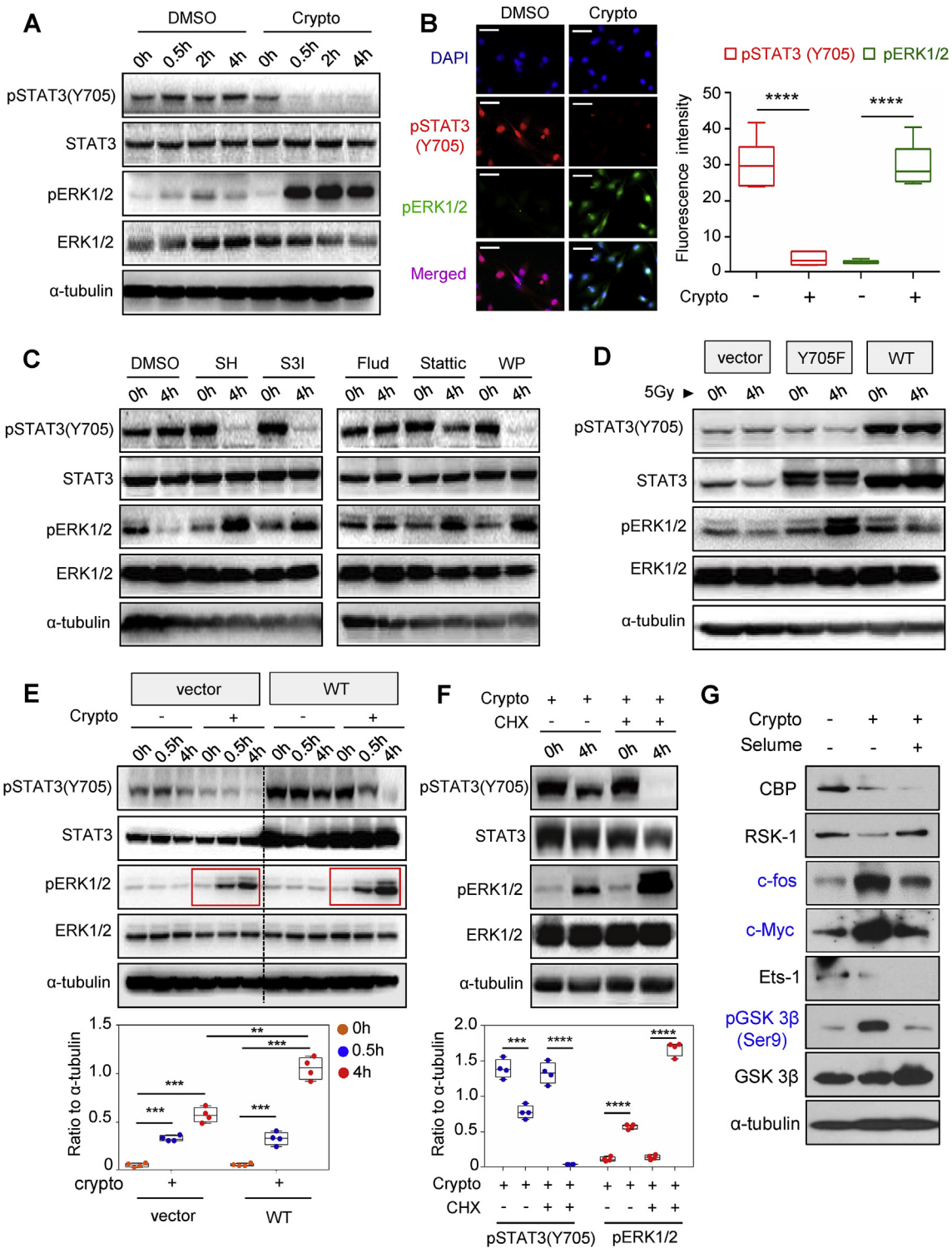

(caption on next page)

To address whether combinational inhibition of STAT3 and ERK1/2 signaling can sensitize radioresistant GBM tumors in vivo. Wild-type U251 cells were subcutaneously injected into nude mice. Tumors reached 200 mm^3 after 16 days inoculation and were exposed to fractionated local RT (2 Gy per day for 5 days). Tumors regressed but regrowth was observed post- RT at day 28. Cryptotanshinone and Selumetinib were then intratumorally injected singly or in combination following a second fractionated RT (2 Gy per day for 2 days). Inhibitors were administered every other day till the end of experiment. After RT, continuous combinative administration of STAT3 and ERK1/2 inhibitors was efficacious in shrinking and delaying tumor regrowth, whereas single agent, on the other hand, revealed limited effect on tumor growth (Fig. 5A–C). In addition to the effect on tumor inhibition, dual administration of inhibitors did not lead to significant mice body weight loss (Fig. 5D). Consistently, dual blockade of STAT3 and ERK1/2 showed the most effective inhibition on the viability of resistant GBM cells while no significant alteration of cell viability was observed in human astrocytes (Supplementary Fig. 8). IHC staining of tumor tissues

Fig. 3. STAT3 inhibition activates ERK1/2 signaling. (**A**) Immunoblotting of pSTAT3 (Y705) and pERK1/2 in U251/C7 cells treated with cryptotanshinone (10 μM) for 0, 0.5, 2 or 4 h. (**B**) Left, representative immunofluorescence of pSTAT3 (Y705) and pERK1/2 in U251/C7 cells treated with DMSO or cryptotanshinone (10 μM) for 4 h. Right, fluorescence intensity of pSTAT3 (Y705) (red box) and pERK1/2 (green box) in cells treated with or without Cryptotanshinone were quantified by ImageJ. Scale bar, 50 μm. (**C**) Immunoblotting of pSTAT3 (Y705) and pERK1/2 in U251/C7 cells after exposure to STAT3 inhibitors SH5-07 (SH, 5 μM), S3I-201 (S3I, 50 μM), Stattic (10 μM) or WP1066 (WP, 5 μM) for 4 h, DMSO and STAT1 inhibitor Fludarabine (Fluid, 10 μM) were used as negative controls. (**D**) Immunoblotting of pERK1/2 in U251/C7 cells transfected with vector, mutant (Y705F) or wild-type STAT3 (WT) 4 h after 5 Gy radiation. (**E**) Above, immunoblotting of pSTAT3 (Y705) and pERK1/2 in U251/C7 cells transfected with vector or wild-type STAT3 and treated with cryptotanshinone (10 μM) for 0.5 h or 4 h. Bottom, the intensity of bands of pERK1/2 in cells transfected with or without wild type STAT3post incubation with Cryptotanshinone 0 h, 0.5 h or 4 h were quantified by ImageJ for 4 times and normalized to α-tubulin. Mean ± SD, $^{**}P < 0.01$, $^{***}P < 0.001$. (**F**) Above, immunoblotting of pSTAT3 (Y705) and pERK1/2 in U251/C7 cells treated with cryptotanshinone (10 μM) in the presence or absence of Cycloheximide (CHX, 20 μg/ml) for 4 h. Bottom, the intensity of bands of pSTAT3(Y705) and pERK1/2 in cells treated with Cryptotanshinone in the presence or absence of CHX were quantified by ImageJ for 4 times and normalized to α-tubulin. Mean ± SD, $^{***}P < 0.001$, $^{****}P < 0.0001$. (**G**) Immunoblotting of CBP, RSK-1, c-fos, c-Myc, Ets-1, phosphorylated GSK 3β (Ser 9) and GSK 3β in U251/C7 cells incubated with cryptotanshinone (10 μM) with or without MEK1/2 inhibitor selumetinib (selume, 1 μM) for 24 h. Data are representative of three independent experiment. (For interpretation of the references to colour in this figure legend, the reader is referred to the Web version of this article.)

from different groups demonstrated enhanced ERK1/2 phosphorylation by STAT3 inhibition which could be blocked via an additional administration of MEK1/2 inhibitor. Combinative inhibition of pSTAT3 (Y705) and pERK1/2 efficiently initiated caspase 3 cascades in the presence of RT (Fig. 5E). Taken together, these findings suggest that ERK1/2 signaling activation due to blocking pSTAT3 (Y705) reflect the heterogenic cancer cells in solid tumor RT, thus dual blockade of STAT3 and ERK1/2 is a potential efficient strategy to sensitize resistant GBM cells to RT (Supplementary Fig. 9).

4. Discussion

Tumor acquired radioresistance remains a major challenge in GBM therapy. The current study reveals a previously unknown heterogenetic feature of radioresistant GBM cells that can survive radiation with STAT3 deficiency due to ERK1/2 activation. This finding is highly informative for understanding the mechanistic insights of GBM resistance and suggests a potentially effective strategy to sensitize resistant GBM cells to radiation by blocking STAT3 and ERK1/2 activation.

With the advent of powerful techniques, optimized preclinical models and increased armory of antitumor drugs, there have now been unprecedented opportunities to unveil the mechanisms of and overcome GBM radioresistance through rational clinical assessments of combinational approaches and developing predictive biomarkers to enable precise patient stratification. STAT3, an oncogenic transcription factor, has been extensively studied and well-defined in cancer responses to therapy and a promising target in cancer treatment [15,16]. STAT3 is shown to be required for maintenance of the stemness of cells derived from human GBM tumor specimens [12] and blocking of STAT3 depleted multipotency, but could not induce apoptosis in GBM stem cells, of which the underlying mechanisms remain unclear. Here we reveal that the radioresistant GBM cells derived from clinically mimic fractionated radiation were enriched with stemness markers which agreed with the recurrent GBM post RT. However, surprisingly, although STAT3 inhibition or even gene deficiency inhibited the majority of cells, a fraction of cells survived from radiation with STAT3 blockade with ERK1/2 activation. In comparison with cells with STAT3 inhibition or CRISPR/cas9-mediated STAT3 knockout, no much difference of CD133 expression was observed in radioresistant GBM cells without treatment, implying that radioresistant GBM cells were able to main the stemness after STAT3 was blocked. Furthermore, tumor spheres grown in medium containing STAT3 inhibitors revealed lager size than those incubated with DMSO. Mechanistic studies demonstrated that ERK1/2 signaling was activated to promote cell survival after pSTAT3 (Y705) was blocked in radioresistant cells. An additional administration of ERK1/2 inhibition could help to eradicate the cells survived STAT3 inhibition and radiation treatment. These results demonstrate a previously unknown heterogenetic GBM cells in which ERK1/2 is essential for surviving not only radiation but also when STAT3 signaling pathway is blocked.

This work further supports the notion that targeting existing activated oncogenic pathways may not achieve efficient anti-tumor effects. A variety of mechanisms involving in drug resistance have been identified in diverse cancer models [48]. Interleukin 6 (IL-6), a multifunctional cytokine regulating cell proliferation and survival through STAT3, was reported to release in the thymus in response to doxorubicin treatment, leading to the survival of lymphoma cells and ultimately patient relapse [49]. Blockade of ERBB2 activated MEK-ERK1/2 signaling was found in ERBB2-amplified breast cancer cells in a HGF-dependent manner [50]. Here, we show that radioresistant GBM cells survive from the combination of radiation and STAT3 blockade via an oncogenic bypass: enhancing ERK1/2 signaling activation, a hidden mechanism unperceived in GBM therapeutic resistance. Our data suggest that this mechanism may be a general “escape-route” for cancers subjected to RT, such as GBM, breast cancer and lung cancer cells.

Another observation potentially related to the clinical scenario is that pSTAT3 (Y705) competitively inhibit ERK1/2 and pSTAT3 (Y705) inhibition activates ERK1/2 leading to disrupt the therapeutic efficacy of STAT3 inhibitors. Accumulating evidence suggests that ERK1/2 signaling can be activated by series inhibitors targeting other oncoproteins essential for tumor progression. ERK1/2 signaling in lung cancer cells with wild-type BRAF can be activated by RAF inhibitors in a RAS-dependent manner [27,51]. RAF inhibitors accelerated the growth of HRAS Q61L-mutant cells of skin-cancer lesions from patients by re-activating ERK1/2 signaling, this growth can be blocked by an additional use of MEK inhibitor [52]. Paradoxical hyperactivation of ERK1/2 signaling was also observed in RAS-mutant leukemia in melanoma patient received BRAF Inhibitor vemurafenib, and was reported to accelerate the proliferation of leukemic cells and reversed by drug withdraw [53]. Additionally, STAT3 activation was triggered by MEK inhibitors administration in an array of oncogene-addicted cancer cells through FGFR and IL-6 signaling and significantly limits the therapeutic efficacy. Disrupting STAT3 feedback activation improved the efficacy of MEK inhibition in vitro and in vivo [20].

In summary, our findings reveal that blocking STAT3 activation with either inhibitors or site mutation activates pro-survival ERK1/2 signaling to prevent cells from apoptosis induced by a combination of STAT3 inhibition and radiation. It is notable that resistant GBM cells and regrown tumors post RT, which actively engage the ERK1/2 activation upon STAT3 inhibition, can be significantly sensitized to an additional ERK1/2 inhibition. Thus, radiation combined with dual blockage of STAT3 and ERK1/2 is a potential effective approach for GBM therapy.

Author contributions

L.S., J.L. and B.X. designed the research. B.X. did the most experiments. W.H. and W.X. performed the experiments of tumor cells transplantation. W.X., B.X., J.L., and K.L. developed the orthotopic NSGGBM model with in vivo radiation and imaging. B.X., L.Z., Y.D., N.J., D.J., J.L. and L.S. acquired and analyzed the data. B.X. wrote the manuscript, L.S., and J.L. proofread and edited the manuscript.

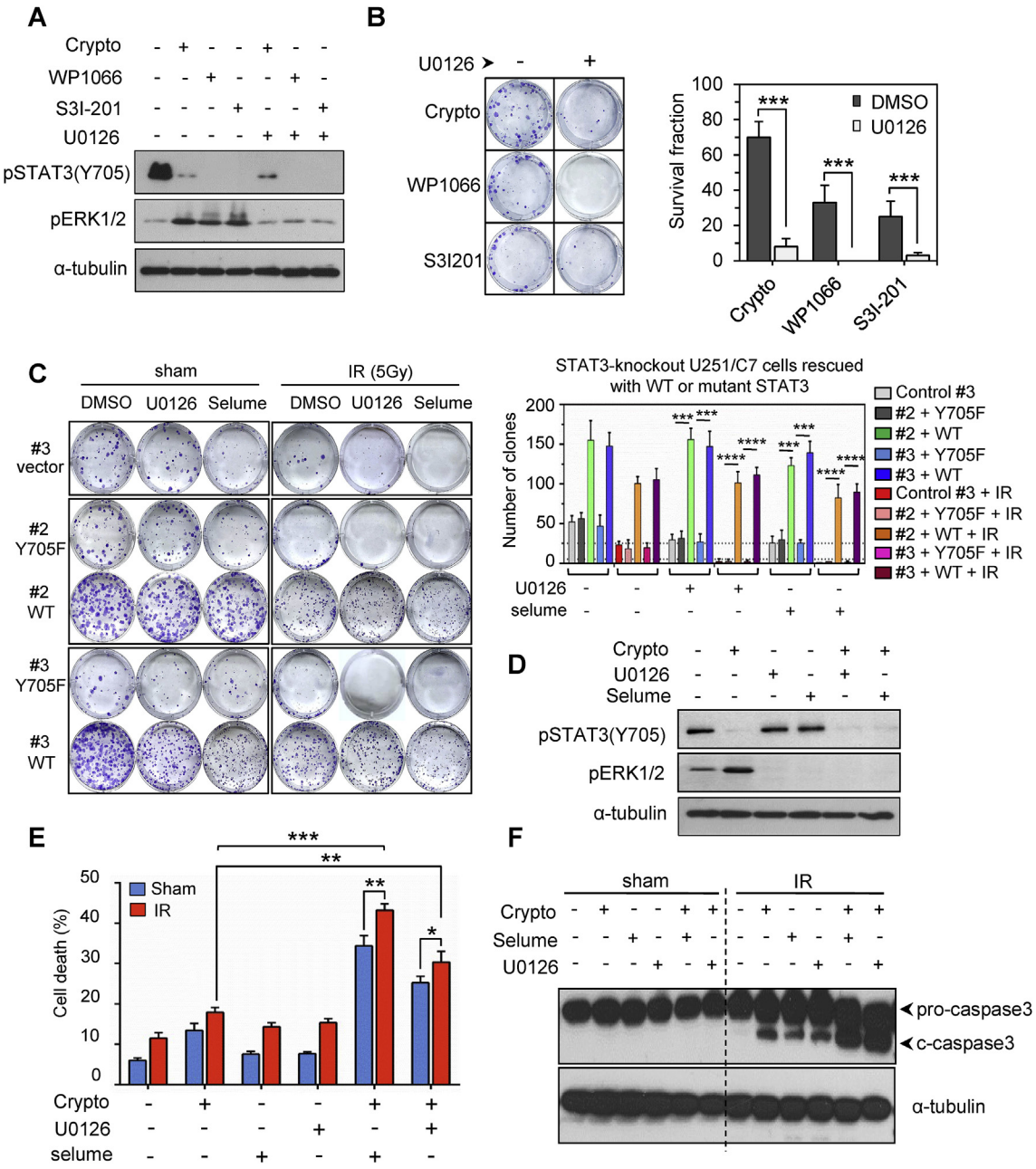

Fig. 4. Enhanced ERK1/2 activation mediates resistance to radiation in GBM cells. (**A**) Immunoblotting of pSTAT3 (Y705) and pERK1/2 in U251/C7 cells exposed to cryptotanshinone (10 μM), WP1066 (5 μM) or S3I-201 (50 μM) for 4 h in the presence or absence of U0126 (10 μM; ERK1/2 inhibition). (**B**) Clonogenic survival of U251/C7 cells. Briefly, cells were incubated with cryptotanshinone (10 μM), WP1066 (5 μM) or S3I-201 (50 μM) for 4 h and then were exposed to 5 Gy radiation. Mean ± SD, ***$P < 0.001$. (**C**) Left, clonogenicity of STAT3-knockout #3 cells rescued with vector, mutant STAT3 (Y705F) or wild-type STAT3, and STAT3 knockout #2 cells rescued with mutant STAT3 (Y705F) or wild-type STAT3. Briefly, cells were incubated with U0126 (5 μM) or selumetinib (selume, 1 μM; ERK1/2 inhibition) and following with exposure to 5 Gy radiation. The survived clones were stained with crystal violet after 12 days cell culture. Right, quantification of the survived clones in each group. Data are shown as the mean values ± SD of triplicates, ***$P < 0.001$, ****$P < 0.0001$. (**D**) Western blot of pSTAT3 (Y705) and pERK1/2 in U251/C7 cells exposed to cryptotanshinone (10 μM) combined with or without U0126 (5 μM) or selumetinib (1 μM) for 4 h. (**E**) Annexin V-FITC and propidium iodide (PI) staining inU251/C7 cells 48 h after exposure to 5 Gy radiation. Before radiation treatment, cells have been pretreated with cryptotanshinone (10 μM) in the presence or absence of selumetinib (1 μM) or U0126 (10 μM) for 4 h. Mean ± SD of triplicates. *$P < 0.05$, **$P < 0.01$, ***$P < 0.001$ (student's *t*-test, two tailed). (**F**) Immunoblotting of cleaved-caspase3 in U251/C7 cells. U251/C7 cells pretreated with cryptotanshinone, selumetinib, U0126 or indicated combinations for 4 h were exposed to 5 Gy radiation for further 24 h. Data are representative of three independent experiment.

Conflicts of interest

The authors declare no conflicts of interest.

Funding

This work was partially supported by National Natural Science Foundation of China (81672509 and 81530084 to L.S.) and the US National Cancer Institute Grants (CA152313 to J.L.). The costs of publication of this article were defrayed in part by the payment of page charges. This article must therefore be hereby marked advertisement in accordance with 18 U. S. C. Section 1734 solely to indicate this fact.

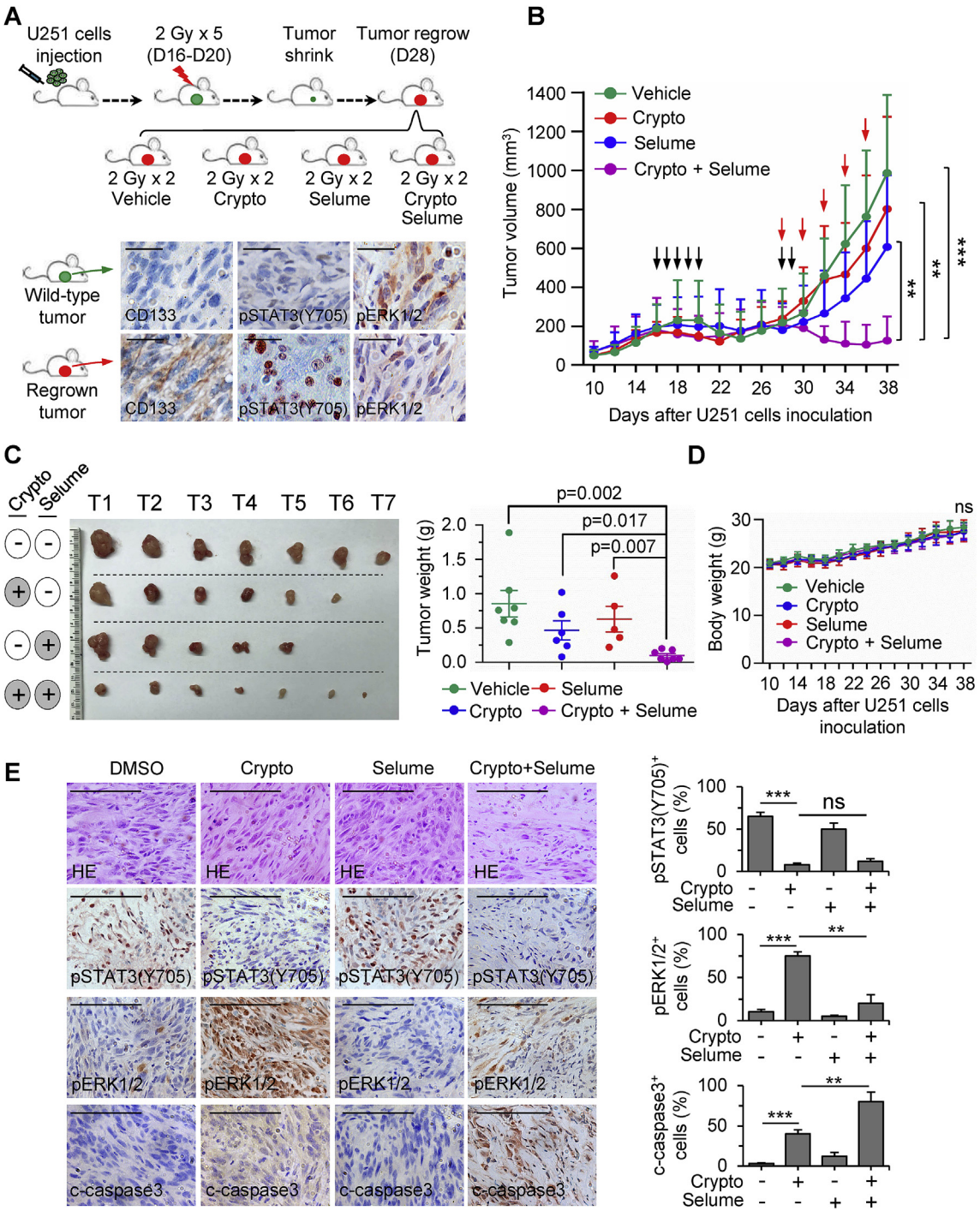

Fig. 5. Dual blockade of STAT3 and ERK1/2 inhibits the regrowth of irradiated GBM tumors. (**A**) Above, tumor regrowth and treatment model were generated with 3×10^6 U251 cells subcutaneously transplanted into nude mice. When tumor volume reached 200 mm^3local radiation was delivered 2 Gy per day for 5 days (from Day 16 to Day 20). At day 28, IHC stain of CD133, pSTAT3 and pERK1/2 were performed in wild type or regrown tumors (bottom), and the regrown tumors were treated with intratumoral injection of DMSO, Cryptotanshinone (Crypto, 25 mg/kg), Selumetinib (Selume, 25 mg/kg) or a combination of Crytotanshinone (25 mg/kg) and Selumetinib (25 mg/kg), and subsequently were exposed to local RT (2 Gy per day for 2 days). Inhibitors were intratumorally injected every other day till the end of experiment. **(B)** Tumor growth in nude mice with indicated treatments. Mean ± SD. $^{**}P < 0.01$, $^{***}P < 0.001$ (student's *t*-test, two tailed). Black arrow, RT; red arrow, inhibitor treatment. (**C**) Image of tumors in each group at the end of experiment (left; n = 7 in DMSO group, n = 6 in Crypto group, n = 5 in Selume group and n = 7 in combination group). Tumor weights (**right**) and mice body weights (**D**) were also recorded. (**E**) HE stain, IHC stain and quantification of pSTAT3 (Y705), pERK1/2 and cleaved-caspase 3 (c-caspase 3) in xenografts from indicated groups. Scale bar, 100 μm. Mean ± SD, ns, no significance, $^{**}P < 0.01$, $^{***}P < 0.001$. (For interpretation of the references to colour in this figure legend, the reader is referred to the Web version of this article.)

Disclosure

Disclosure of Potential Conflicts of Interest.

Acknowledgements

We acknowledge Dr. Hongwu Chen at University of California Davis School of Medicine for the discussion and for the assistance of CRIPR/Cas9 technology, respectively.

Appendix A. Supplementary data

Supplementary data to this article can be found online at https://doi.org/10.1016/j.redox.2019.101189.

References

[1] F. Keime-Guibert, O. Chinot, L. Taillandier, S. Cartalat-Carel, M. Frenay, G. Kantor, et al., Radiotherapy for glioblastoma in the elderly, N. Engl. J. Med. 356 (2007) 1527–1535.
[2] R. Stupp, W.P. Mason, M.J. van den Bent, M. Weller, B. Fisher, M.J. Taphoorn, et al., Radiotherapy plus concomitant and adjuvant temozolomide for glioblastoma, N. Engl. J. Med. 352 (2005) 987–996.
[3] M. Baumann, M. Krause, R. Hill, Exploring the role of cancer stem cells in radioresistance, Nat. Rev. Cancer 8 (2008) 545–554.
[4] K.P.L. Bhat, V. Balasubramaniyan, B. Vaillant, R. Ezhilarasan, K. Hummelink, F. Hollingsworth, et al., Mesenchymal differentiation mediated by NF-kappaB promotes radiation resistance in glioblastoma, Cancer Cell 24 (2013) 331–346.
[5] N. Uchida, D.W. Buck, D. He, M.J. Reitsma, M. Masek, T.V. Phan, et al., Direct isolation of human central nervous system stem cells, Proc. Natl. Acad. Sci. U. S. A. 97 (2000) 14720–14725.
[6] S.K. Singh, C. Hawkins, I.D. Clarke, J.A. Squire, J. Bayani, T. Hide, et al., Identification of human brain tumour initiating cells, Nature 432 (2004) 396–401.
[7] R.D. Carruthers, S.U. Ahmed, S. Ramachandran, K. Strathdee, K.M. Kurian, A. Hedley, et al., Replication stress drives constitutive activation of the DNA damage response and radioresistance in glioblastoma stem-like cells, Cancer Res. 78 (2018) 5060–5071.
[8] S. Bao, Q. Wu, R.E. McLendon, Y. Hao, Q. Shi, A.B. Hjelmeland, et al., Glioma stem cells promote radioresistance by preferential activation of the DNA damage response, Nature 444 (2006) 756–760.
[9] S. Haga, K. Terui, H.Q. Zhang, S. Enosawa, W. Ogawa, H. Inoue, et al., Stat3 protects against Fas-induced liver injury by redox-dependent and -independent mechanisms, J. Clin. Investig. 112 (2003) 989–998.
[10] L. Li, S.H. Cheung, E.L. Evans, P.E. Shaw, Modulation of gene expression and tumor cell growth by redox modification of STAT3, Cancer Res. 70 (2010) 8222–8232.
[11] S. Paul, A. Gangwar, K. Bhargava, Y. Ahmad, STAT3-RXR-Nrf2 activates systemic redox and energy homeostasis upon steep decline in pO2 gradient, Redox. Biol. 14 (2018) 423–438.
[12] M.M. Sherry, A. Reeves, J.K. Wu, B.H. Cochran, STAT3 is required for proliferation and maintenance of multipotency in glioblastoma stem cells, Stem Cells 27 (2009) 2383–2392.
[13] C. Won, B.H. Kim, E.H. Yi, K.J. Choi, E.K. Kim, J.M. Jeong, et al., Signal transducer and activator of transcription 3-mediated CD133 up-regulation contributes to promotion of hepatocellular carcinoma, Hepatology 62 (2015) 1160–1173.
[14] T. Gritsko, A. Williams, J. Turkson, S. Kaneko, T. Bowman, M. Huang, et al., Persistent activation of stat3 signaling induces survivin gene expression and confers resistance to apoptosis in human breast cancer cells, Clin. Cancer Res. 12 (2006) 11–19.
[15] T.X. Xie, F.J. Huang, K.D. Aldape, S.H. Kang, M. Liu, J.E. Gershenwald, et al., Activation of stat3 in human melanoma promotes brain metastasis, Cancer Res. 66 (2006) 3188–3196.
[16] H. Yu, D. Pardoll, R. Jove, STATs in cancer inflammation and immunity: a leading role for STAT3, Nat. Rev. Cancer 9 (2009) 798–809.
[17] M.S. Carro, W.K. Lim, M.J. Alvarez, R.J. Bollo, X. Zhao, E.Y. Snyder, et al., The transcriptional network for mesenchymal transformation of brain tumours, Nature 463 (2010) 318–325.
[18] O.A. Guryanova, Q. Wu, L. Cheng, J.D. Lathia, Z. Huang, J. Yang, et al., Nonreceptor tyrosine kinase BMX maintains self-renewal and tumorigenic potential of glioblastoma stem cells by activating STAT3, Cancer Cell 19 (2011) 498–511.
[19] H. Korkaya, G.I. Kim, A. Davis, F. Malik, N.L. Henry, S. Ithimakin, et al., Activation of an IL6 inflammatory loop mediates trastuzumab resistance in HER2+ breast cancer by expanding the cancer stem cell population, Mol. Cell 47 (2012) 570–584.
[20] H.J. Lee, G. Zhuang, Y. Cao, P. Du, H.J. Kim, J. Settleman, Drug resistance via feedback activation of Stat3 in oncogene-addicted cancer cells, Cancer Cell 26 (2014) 207–221.
[21] S.M. Kim, O.J. Kwon, Y.K. Hong, J.H. Kim, F. Solca, S.J. Ha, et al., Activation of IL-6R/JAK1/STAT3 signaling induces de novo resistance to irreversible EGFR inhibitors in non-small cell lung cancer with T790M resistance mutation, Mol. Cancer Therapeut. 11 (2012) 2254–2264.
[22] B. Dai, J. Meng, M. Peyton, L. Girard, W.G. Bornmann, L. Ji, et al., STAT3 mediates resistance to MEK inhibitor through microRNA miR-17, Cancer Res. 71 (2011) 3658–3668.
[23] D. Kesanakurti, C. Chetty, D. Rajasekhar Maddirela, M. Gujrati, J.S. Rao, Essential role of cooperative NF-kappaB and Stat3 recruitment to ICAM-1 intronic consensus elements in the regulation of radiation-induced invasion and migration in glioma, Oncogene 32 (2013) 5144–5155.
[24] Y.P. Yang, Y.L. Chang, P.I. Huang, G.Y. Chiou, L.M. Tseng, S.H. Chiou, et al., Resveratrol suppresses tumorigenicity and enhances radiosensitivity in primary glioblastoma tumor initiating cells by inhibiting the STAT3 axis, J. Cell. Physiol. 227 (2012) 976–993.
[25] T.J. Han, B.J. Cho, E.J. Choi, D.H. Kim, S.H. Song, S.H. Paek, et al., Inhibition of STAT3 enhances the radiosensitizing effect of temozolomide in glioblastoma cells in vitro and in vivo, J. Neuro Oncol. 130 (2016) 89–98.
[26] K.S. Saini, S. Loi, E. de Azambuja, O. Metzger-Filho, M.L. Saini, M. Ignatiadis, et al., Targeting the PI3K/AKT/mTOR and Raf/MEK/ERK pathways in the treatment of breast cancer, Cancer Treat Rev. 39 (2013) 935–946.
[27] G. Hatzivassiliou, K. Song, I. Yen, B.J. Brandhuber, D.J. Anderson, R. Alvarado, et al., RAF inhibitors prime wild-type RAF to activate the MAPK pathway and enhance growth, Nature 464 (2010) 431–435.
[28] G.W. Booz, J.N. Day, K.M. Baker, Angiotensin II effects on STAT3 phosphorylation in cardiomyocytes: evidence for Erk-dependent Tyr705 dephosphorylation, Basic Res. Cardiol. 98 (2003) 33–38.
[29] N. Jain, T. Zhang, S.L. Fong, C.P. Lim, X. Cao, Repression of Stat3 activity by activation of mitogen-activated protein kinase (MAPK), Oncogene 17 (1998) 3157–3167.
[30] S. You, R. Li, D. Park, M. Xie, G.L. Sica, Y. Cao, et al., Disruption of STAT3 by niclosamide reverses radioresistance of human lung cancer, Mol. Cancer Therapeut. 13 (2014) 606–616.
[31] Z. Wang, M. Fan, D. Candas, T.Q. Zhang, L. Qin, A. Eldridge, et al., Cyclin B1/Cdk1 coordinates mitochondrial respiration for cell-cycle G2/M progression, Dev. Cell 29 (2014) 217–232.
[32] C.R. Yu, L. Wang, A. Khaletskiy, W.L. Farrar, A. Larner, N.H. Colburn, et al., STAT3 activation is required for interleukin-6 induced transformation in tumor-promotion sensitive mouse skin epithelial cells, Oncogene 21 (2002) 3949–3960.
[33] J. Wang, J.X. Zou, X. Xue, D. Cai, Y. Zhang, Z. Duan, et al., ROR-gamma drives androgen receptor expression and represents a therapeutic target in castration-resistant prostate cancer, Nat. Med. 22 (2016) 488–496.
[34] K. Shimozaki, K. Nakajima, T. Hirano, S. Nagata, Involvement of STAT3 in the granulocyte colony-stimulating factor-induced differentiation of myeloid cells, J. Biol. Chem. 272 (1997) 25184–25189.
[35] T. Gao, F. Furnari, A.C. Newton, PHLPP: a phosphatase that directly dephosphorylates Akt, promotes apoptosis, and suppresses tumor growth, Mol. Cell 18 (2005) 13–24.
[36] C. Wang, L. Chen, X. Hou, Z. Li, N. Kabra, Y. Ma, et al., Interactions between E2F1 and SirT1 regulate apoptotic response to DNA damage, Nat. Cell Biol. 8 (2006) 1025–1031.
[37] M. Das Thakur, F. Salangsang, A.S. Landman, W.R. Sellers, N.K. Pryer, M.P. Levesque, et al., Modelling vemurafenib resistance in melanoma reveals a strategy to forestall drug resistance, Nature 494 (2013) 251–255.
[38] R. Buettner, L.B. Mora, R. Jove, Activated STAT signaling in human tumors provides novel molecular targets for therapeutic intervention, Clin. Cancer Res. 8 (2002) 945–954.
[39] S.O. Rahaman, P.C. Harbor, O. Chernova, G.H. Barnett, M.A. Vogelbaum, S.J. Haque, Inhibition of constitutively active Stat3 suppresses proliferation and induces apoptosis in glioblastoma multiforme cells, Oncogene 21 (2002) 8404–8413.
[40] D.S. Shin, H.N. Kim, K.D. Shin, Y.J. Yoon, S.J. Kim, D.C. Han, et al., Cryptotanshinone inhibits constitutive signal transducer and activator of transcription 3 function through blocking the dimerization in DU145 prostate cancer cells, Cancer Res. 69 (2009) 193–202.
[41] L. Zhou, Z. Zuo, M.S. Chow, Danshen: an overview of its chemistry, pharmacology, pharmacokinetics, and clinical use, J. Clin. Pharmacol. 45 (2005) 1345–1359.
[42] A. Ferrajoli, S. Faderl, Q. Van, P. Koch, D. Harris, Z. Liu, et al., WP1066 disrupts Janus kinase-2 and induces caspase-dependent apoptosis in acute myelogenous leukemia cells, Cancer Res. 67 (2007) 11291–11299.
[43] A. Horiguchi, T. Asano, K. Kuroda, A. Sato, J. Asakuma, K. Ito, et al., STAT3 inhibitor WP1066 as a novel therapeutic agent for renal cell carcinoma, Br. J. Cancer 102 (2010) 1592–1599.
[44] P. Wang, Y. Xue, Y. Han, L. Lin, C. Wu, S. Xu, et al., The STAT3-binding long noncoding RNA lnc-DC controls human dendritic cell differentiation, Science 344 (2014) 310–313.
[45] M.R. Girotti, M. Pedersen, B. Sanchez-Laorden, A. Viros, S. Turajlic, D. Niculescu-Duvaz, et al., Inhibiting EGF receptor or SRC family kinase signaling overcomes BRAF inhibitor resistance in melanoma, Cancer Discov. 3 (2013) 158–167.
[46] B. Magnuson, B. Ekim, D.C. Fingar, Regulation and function of ribosomal protein S6 kinase (S6K) within mTOR signalling networks, Biochem. J. 441 (2012) 1–21.
[47] R.K. Lo, H. Wise, Y.H. Wong, Prostacyclin receptor induces STAT1 and STAT3 phosphorylations in human erythroleukemia cells: a mechanism requiring PTX-insensitive G proteins, ERK and JNK, Cell. Signal. 18 (2006) 307–317.
[48] C. Holohan, S. Van Schaeybroeck, D.B. Longley, P.G. Johnston, Cancer drug resistance: an evolving paradigm, Nat. Rev. Cancer 13 (2013) 714–726.
[49] L.A. Gilbert, M.T. Hemann, DNA damage-mediated induction of a chemoresistant niche, Cell 143 (2010) 355–366.
[50] E. Greenfield, E. Griner, Reproducibility Project: cancer B. Registered report: widespread potential for growth factor-driven resistance to anticancer kinase inhibitors, Elife 3 (2014).

[51] P.I. Poulikakos, C. Zhang, G. Bollag, K.M. Shokat, N. Rosen, RAF inhibitors transactivate RAF dimers and ERK signalling in cells with wild-type BRAF, Nature 464 (2010) 427–430.
[52] F. Su, A. Viros, C. Milagre, K. Trunzer, G. Bollag, O. Spleiss, et al., RAS mutations in cutaneous squamous-cell carcinomas in patients treated with BRAF inhibitors, N. Engl. J. Med. 366 (2012) 207–215.
[53] M.K. Callahan, R. Rampal, J.J. Harding, V.M. Klimek, Y.R. Chung, T. Merghoub, et al., Progression of RAS-mutant leukemia during RAF inhibitor treatment, N. Engl. J. Med. 367 (2012) 2316–2321.